Available online at www.sciencedirect.com
SCIENCE DIRECT
Journal of Virological Methods 129 (2005) 145–151
Journal of Virological Methods
www.elsevier.com/locate/jviromet

Spectroscopic analysis of Kaposi's sarcoma-associated herpesvirus infected cells by Raman tweezers

Khalief E. Hamden [a], Benjaman A. Bryan [a], Patrick W. Ford [a], Changan Xie [b], Yong-Qing Li [b], Shaw M. Akula [a,*]

[a] *Department of Microbiology & Immunology, Brody School of Medicine, East Carolina University, Greenville, NC 27834, USA*
[b] *Department of Physics, East Carolina University, Greenville, NC 27858, USA*

Received 28 February 2005; received in revised form 12 May 2005; accepted 16 May 2005
Available online 29 June 2005

Abstract

Kaposi's sarcoma-associated herpesvirus (KSHV), also referred to as human herpesvirus-8 (HHV-8), is a tumor causing virus. KSHV is the cause of several disease conditions known as Kaposi's sarcoma, multicentric Castleman disease, and primary effusion lymphoma. Cell culture supernatants from KSHV infected hematopoietic cells induced angiogenic tubule formation to a significantly greater extent than uninfected hematopoietic cells. Raman spectrum profiles were generated to differentiate the uninfected from KSHV infected cells. In general, profiles from all the hematopoietic cells shared similar peaks; however, the relative abundance of specific components varied significantly between the cells. Subsequent use of the multivariate analysis of the Raman spectra revealed significant differences between the uninfected and the KSHV infected cells. Taken together, this study reports the use of Raman tweezers to distinguish and analyze the biological relevance of KSHV infected cell signaling.

Keywords: KSHV; HHV-8; VEGF; Raman tweezers; Spectroscopy

1. Introduction

Kaposi's sarcoma-associated herpesvirus (KSHV/HHV-8) is associated etiologically with Kaposi's sarcoma, multicentric Castleman disease, and primary effusion lymphoma (Chang et al., 1994). Since its discovery in 1994, the entire virus genome has been sequenced successfully (Neipel et al., 1997; Russo et al., 1996). Raf has been identified as an oncogene in a variety of human cancers (Davies et al., 2002; Karasarides et al., 2004; Kimura et al., 2003; Mercer and Pritchard, 2003). Constitutive activation of the components (Ras/Raf) of the MAPK pathway of signaling has been associated with a variety of tumors; including AIDS-related KS (Faris et al., 1996). Oncoprotein Raf enhances KSHV infection of target cells (Akula et al., 2004); more importantly, Raf also regulates expression of vascular endothelial growth factor (VEGF) (Ensoli et al., 2001; Hamden et al., 2004, 2005; Weinstein-Oppenheimer et al., 2002); VEGF is a key factor in KSHV mediated pathogenesis due to its role in angiogenesis (Ensoli et al., 2001).

The three principal features of KS tumors are angiogenesis, inflammation, and proliferation (Gallo, 1998). In a study concluded recently, KSHV infected hematopoietic cells (BCBL-1 and BC-1 cells) were demonstrated to express elevated levels of B-Raf kinase activity and VEGF when compared to uninfected BJAB cells (Akula et al., 2005). Inhibition of either B-Raf or VEGF expression in BCBL-1 and BC-1 cells by small interfering RNAs (SiRNA) lowered specifically the ability of cell culture supernatant to induce tubule formation in endothelial cells (Akula et al., 2005). However, knowledge of the role for KSHV infection of these cells in mediating angiogenic tubule formation is lacking. Hence, in this study the ability of cell culture supernatants derived from uninfected and KSHV infected cells to support tubule formation in endothelial cells was compared. In addition, Raman

* Corresponding author. Tel.: +1 252 744 2702; fax: +1 252 744 3104.
E-mail address: akulas@mail.ecu.edu (S.M. Akula).

0166-0934/$ – see front matter © 2005 Elsevier B.V. All rights reserved.
doi:10.1016/j.jviromet.2005.05.018

tweezers was used to delineate the differences between the uninfected and KSHV infected cells.

2. Materials and methods

2.1. Cells

BCBL-1, BC-1, and BJAB cells were cultured in phenol red-free RPMI medium (Invitrogen, Carlsbad, CA, USA) containing 5% charcoal stripped fetal bovine serum (FBS) (Atlanta Biologicals Inc., Lawrenceville, GA, USA), L-glutamine, and antibiotics as per standard protocols (Akula et al., 2005). Dermal microvascular endothelial cells (HMVEC-d; CC-2543, Clonetics) were propagated in EGM™ MV-microvascular endothelial cell medium (Clonetics) as per standard protocols (Akula et al., 2002). The passage number for HMVEC-d cells used in this study ranged between 5 and 9.

2.2. Reverse transcriptase PCR (RT-PCR)

RT-PCR to monitor KSHV infection of cells was carried out according to standard protocols mentioned earlier (Akula et al., 2004).

2.3. In vitro angiogenesis assay

The formation of capillary tube-like structures by HMVEC-d cells was analyzed on tumor-derived basement membrane matrix (Matigel, Discovery Labware, Bedford, MA). Ninety-six-well culture dishes were coated with 80 μl per well of Matrigel on ice. Matrigel was allowed to polymerize for 30 min at 37 °C. HMVEC-d cells were trypsinized and washed once in growth medium at 400 × *g*, 10 min, +4 °C. The cells were washed again in 10 ml of RPMI. These cells (1×10^4) were resuspended in 100 μl of RPMI containing 2% FBS, RPMI containing 2% FBS and 5 ng ml^{-1} of VEGF (R&D Systems, Inc., Minneapolis, MN), or test samples and were seeded into respective Matrigel-coated wells. The test samples included the conditioned medium obtained from BCBL-1, BC-1, and BJAB cells. Conditioned medium refers to medium (RPMI containing 2% FBS) collected 48 h post culturing cells. After 16 h incubation at 37 °C, the cells were labeled with calcein AM (Invitrogen) as per the manufacturer's recommendations. Endothelial tubule formation by the cells was observed under an Olympus IMT-2 inverted microscope and tubular structures were scored by counting the number of tubules in each well (Liu et al., 2002). Tubules shorter than 100 μm were excluded from the measurement.

2.4. Raman tweezers, spectra acquisition, and data processing

A detailed description of the Raman tweezers is provided in the legend for Fig. 1 (Xie and Li, 2003). Raman spectra for the different target cells were acquired using a spectrograph (Triax 320, Jobin Yvon Ltd., Edson, NJ) equipped with a liquid nitrogen cooled CCD detector. Raman signal was collected in the spectral interval from 400 to 2100 cm^{-1} with a resolution of 6 cm^{-1}. Spectral acquisition for each cell was performed with a collection time of 60 s, 20 mW at 780 nm. All the cells analyzed by this procedure were suspended in RPMI containing 5% FBS. Each individual cell was held in the laser beam and elevated from the cover slide about 10 μm to reduce the Brownian motion of the cell during the Raman acquisition and to reduce the fluorescence background from the glass cover slide. The Raman spectra of 20 cells were acquired for each cell type. Fresh samples were used after acquisition of data for 10 cells. The background was recorded with the same acquisition conditions without trapping cells. Following spectral acquisition, the background signal originating from the cover slide and the surrounding medium was subtracted from all the spectra. The subtracted spectra were calibrated with the spectral response function of the Raman system.

2.5. Multivariate analysis of Raman spectra

To analyze the Raman spectra obtained from the hematopoietic cells, multivariate statistical technique of the principal component analysis (PCA) was used as per standard protocols (Huang et al., 2004). Briefly, the spectral data processing involved taking the first derivative of the Raman spectra, performing normalization, and using the 600–1800 cm^{-1} spectral region for further PCA using the Matlab 6.5, PLS toolbox. Normalization is scaling of the spectra to achieve a constant area under the spectroscopic curve, for better comparison. The scores of the first three principal components were used to discriminate the uninfected and infected cells. In the process of doing PCA analysis, 15 cells were used to form a training group for building eigenvectors and calculating the associated scores. The extra five cells of each cell type were then used as the testing group to validate the PCA analysis.

3. Results

First, reverse transcriptase-PCR (RT-PCR) was undertaken to confirm KSHV infection of the above cells and to eliminate possible cross contamination of cells. There was no ORF73 expression in BJAB cells, while both BCBL-1 and BC-1 cells expressed ORF73 indicating KSHV infection of cells (Fig. 2). No detectable signal was observed with reactions carried out in the absence of RT or with no template (Fig. 2), demonstrating the specificity of the RT-PCR performed.

Second, the ability of cell culture supernatants derived from the above hematopoietic cells to support angiogenesis on a Matrigel was tested (Ito et al., 2003). The formation of capillary tube-like structures by HMVEC-d cells

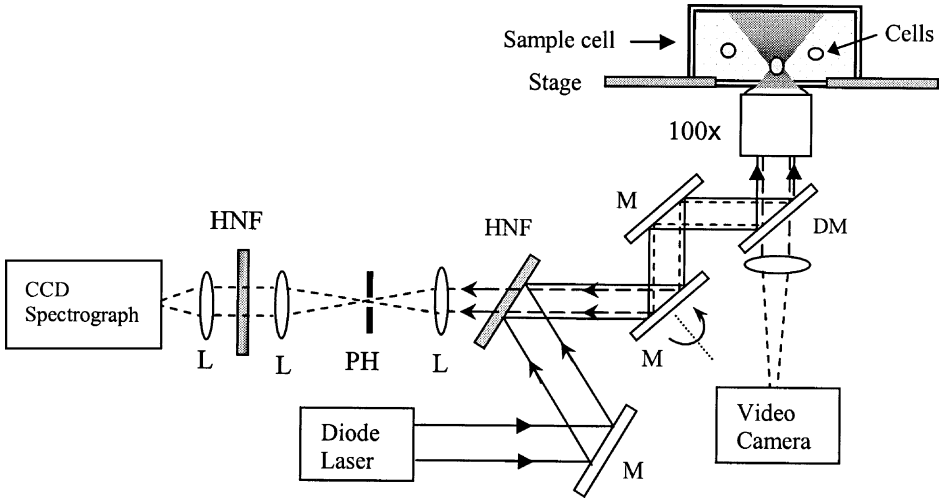

Fig. 1. Raman tweezers. The combined laser tweezers and Raman spectroscopy instrument possesses a laser beam at 785 nm from a wavelength-stabilized, beam shape-circulated semiconductor diode laser that is introduced into an inverted microscope (Nikon 2000S) through a high numerical aperture objective (100×, NA = 1.30) to form an optical trap. The same laser beam can be used to excite Raman scattering of the trapped particle. The scattering light from the particle is collected by the objective and coupled into a spectrograph through a 200 μm pinhole, which enables confocal detection and rejection of off-focusing Rayleigh scattering light. A holographic notch filter is used as a dichroic beam splitter that reflects the 785 nm excitation beam and transmits the Raman shifted light. A green-filtered illumination lamp and a video camera system are used to verify trapping and observe the image of the cell. The spectrograph is equipped with a liquid-nitrogen-cooled charge-coupled detector (CCD). The spectral resolution of our confocal Raman system is about 6 cm^{-1}. *Abbreviations*: M, mirror; L, lens; DM, dichroic mirror; PH, pinhole; HNF, holograph notch filter.

on the tumor-derived basement membrane matrix, Matrigel was considered as the yardstick to monitor angiogenesis. HMVEC-d cells grown on Matrigel supplemented with conditioned medium from BCBL-1 and BC-1 cells significantly induced angiogenic tubule formation when compared to those obtained from BJAB (Fig. 3A–C). Tubule formation in cells was observed when grown in RPMI supplemented with 2% FBS and 5 ng ml^{-1} of VEGF (data not shown), when compared to those grown in RPMI supplemented with just 2% FBS (Fig. 3D and E). Conditioned medium obtained from BJAB cells also induced tubule formation in HMVEC-d cells grown on Matrigel, but the length of the tubules were shorter and less pronounced (Fig. 3C and E). Overall, the cell culture supernatant from KSHV infected cells induced tubule formation to a significantly greater extent when compared to uninfected cells.

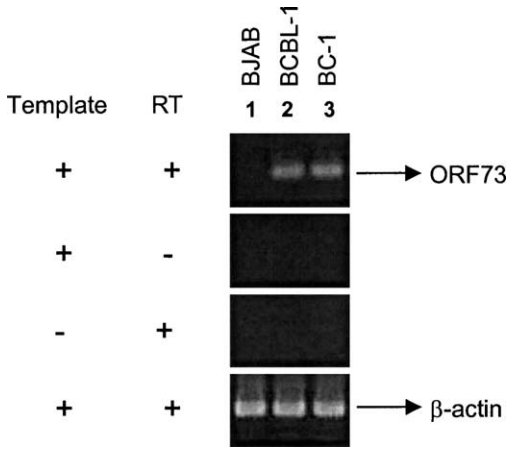

Fig. 2. BCBL-1 and BC-1 cells are infected while BJAB is uninfected. KSHV infection of target cells was monitored by RT-PCR to detect expression of ORF73 (encodes for latency associated nuclear antigen). Briefly, target cells were washed twice in RPMI and incubated at 37 °C in growth medium. After 48 h, total RNA was isolated from cells and examined for viral RNA transcripts by RT-PCR. At the end of 35 cycles of PCR-amplification, the products (ORF73-307 bp; actin-838 bp) were resolved in a 1.2% agarose gel and stained by ethidium bromide.

Finally, Raman tweezers was used to obtain the fingerprints of these cells by measuring the vibrational energy levels without chemically interfering. As Raman tweezers is not a familiar technique to virologists/biologists; a brief descrip-

Table 1
Raman bands for human B cells and their assignments

Bands (cm^{-1})	Assigned component
1663	Amide I
1612	Trp/Tyr/Phe
1581	Nucleic acids (A, G)
1452	Lipid/P (—CH; def)
1343	Nucleic acids (A, G; def)
1320	Nucleic acids (A)
1254	Amide III
1128	C—N
1096	DNA:BK
1032	Phe
1004	Phe
934	DNA:BK
852	Tyr
782	Nucleic acids (C, T)
728	Adenine

Abbreviation: P: protein, BK: the backbone of DNA, def: the deformed vibration of the C—H bond due to the local micro-environmental change.

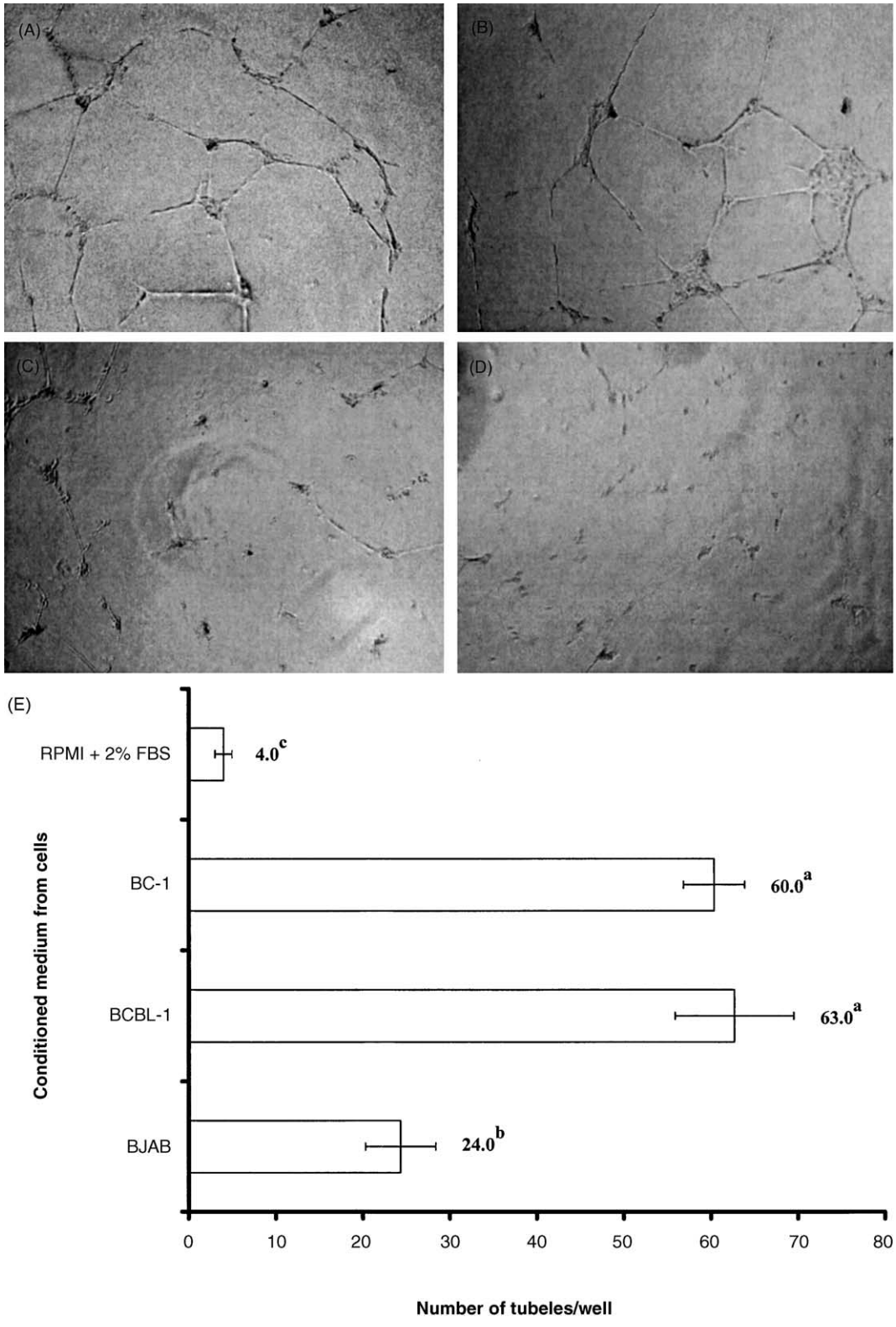

Fig. 3. Conditioned medium from KSHV infected cells induced significantly greater number of tubule formation on Matrigel. HMVEC-d cells cultured on Matrigel-coated wells were analyzed for the ability to form tubules when grown for 16 h in conditioned medium obtained from (A) BCBL-1, (B) BC-1, (C) BJAB cells, and (D) RPMI containing 2% FBS, respectively. Representative illustrations (A–D) are at a magnification of 40×. (E) The tubular structures were scored by counting the number of tubules formed by HMVEC-d cells in each well when grown in conditioned medium from culturing various target cells. Each reaction was done in triplicate, and each point represents the average ± S.D. of three experiments. Average values on the columns with different superscripts are statistically significant ($P < 0.05$) by least significant difference (L.S.D.).

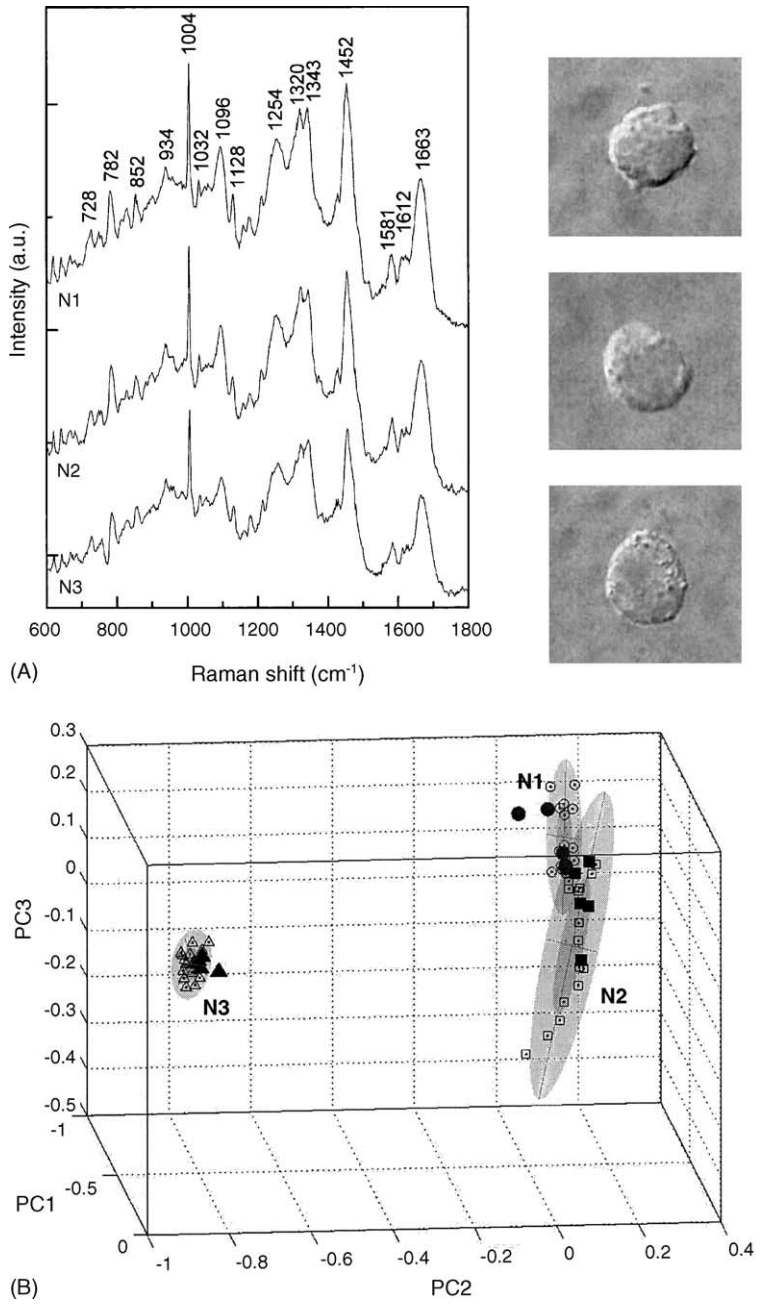

Fig. 4. (A) Raman spectra for different hematopoietic cells. The Raman spectra of different target cells in growth medium (RPMI containing 5% FBS) at 22 °C was acquired. The spectra are an average of data from 20 cells. Cell type N1, N2, and N3 represent BCBL-1, BC-1, and BJAB, respectively. The respective cell for each spectrum is illustrated to the right (100× magnification). (B) Multivariate analysis of Raman spectra differentiates KSHV infected (BCBL-1 and BC-1) from uninfected (BJAB) hematopoietic cells. Multivariate statistical technique of PCA was used as per standard protocols (Huang et al., 2004). Cell type: N1 represents BCBL-1 ((◯) training cells, (●) testing cells); N2 for BC-1 ((□) training cells, (■) testing cells); N3 for BJAB ((△) training cells, (▲) testing cells). The outermost gray ellipsoids represent 90% confidence intervals for the three clusters.

Table 2
Summary of the biochemical and spectroscopic analyses of the hematopoietic cells

Cell type	KSHV	EBV	B-Raf	ERK	VEGF	Tubule formation	Intensities of Raman bands (1004, 1093, and 1664 cm^{-1})
BCBL-1	+	–	++++	++++	++++	++++	++++
BC-1	+	+	++++	++++	++++	++++	++++
BJAB	–	–	++	++	++	++	++

Note: (+) and (–) indicate positive and negative for KSHV infection, respectively. Data provided is based on our previous (Akula et al., 2005) and the present study.

tion may be useful to the readers. Over the years, optical tweezers has been perfected to also study single cells apart from other uses (Ashkin, 1997). Raman tweezers involves a confocal microscopy, which incorporates the use of both laser (optical) tweezers and Raman spectroscopy (LTRS). Very recently, Raman tweezers have also been applied in the study of single cells (Xie et al., 2002; Xie and Li, 2003). Optical tweezers is a technique that utilizes a focused near-infrared laser beam to capture a single biological particle without physically touching it, while Raman spectroscopy uses the same laser beam to analyze the optical spectrum of the cell from the scattering light. The experimental set up for the Raman tweezers is described in the legend for Fig. 1. Each of these cells was trapped optically and analyzed using Raman tweezers. The cells have a rounded morphology with an average diameter of 8–12 μm. For each cell type, the Raman acquisition was done only for the nuclei portion of those cells with the confocal LTRS system. Table 1 lists the Raman bands observed for the hematopoietic cells. The Raman spectrum of BJAB, BCBL-1, and BC-1 cells under physiological conditions was recorded at 22 °C. Among the other subtle differences, the intensities of the Raman bands at 1004, 1093, and 1664 cm^{-1} were significantly altered in the nucleus of KSHV infected cells when compared to uninfected cells. The intensities of the Raman bands at 1004, 1093, and 1664 cm^{-1} were greater in KSHV infected cells (BCBL-1 and BC-1) when compared to uninfected cells (BJAB) (Fig. 4A). The Raman bands at 1004, 1093, and 1664 cm^{-1} represent the side-chain bond (predominantly phenylalanine) of proteins, backbone of nucleic acids, and amide I main-chain of proteins, respectively. Overall, there was a significant increase in the intensities of bands corresponding to proteins and nucleic acids in the KSHV infected cells when compared to the uninfected cells. In addition, a differential clustering pattern was observed between uninfected and KSHV infected cells as analyzed by the multivariant analysis (Fig. 4B).

4. Discussion

All three cells used in this study are of B cell lineage. The only difference is that the BCBL-1 and BC-1 cells are KSHV infected while BJAB is uninfected. One common feature of BCBL-1 and BC-1 cells is that they harbor KSHV, predominantly in latent form with no active replication of virus (Renne et al., 1998). However, the results from previous studies demonstrate KSHV infected hematopoietic cells to express elevated levels of B-Raf kinase > ERK1/2 activity > VEGF expression when compared to the uninfected cells (Akula et al., 2005; Aoki and Tosato, 2001). B-Raf induced VEGF expression was one of the players critical for the tubule formation (Akula et al., 2005). The results from the present study indicates the ability of culture supernatant from KSHV infected cells to support enhanced tubule formation when compared to the supernatant from the uninfected cells (Table 2); implicating indirectly KSHV infection of target cells to play a critical role in the angiogenic tubule formation. Next, the ability of Raman tweezers to differentiate between the uninfected and KSHV infected cells was analyzed.

Data from this study revealed the potential of Raman tweezers to detect differences in the physiological state of uninfected cells from KSHV infected cells. The significant increase in the intensity of 1004, 1093, and 1664 cm^{-1} bands in infected cells over the uninfected cells is probably due to the cellular changes induced by the KSHV infection of cells. Accordingly, there was a differential clustering pattern observed between uninfected and KSHV infected cells as analyzed by the multivariant analysis (Fig. 4B). These results are interesting given the fact that BCBL-1, BC-1, and BJAB are human B cells derived from lymphomas (Table 2): BCBL-1 and BC-1 cells are infected with KSHV and derived from primary effusion lymphoma patients (Ablashi et al., 2002), while BJAB cells are uninfected and derived from Burkitts lymphoma (Zhang and Nonoyama, 1994). These cells are routinely used to study KSHV and mediated pathogenesis (Lagunoff et al., 2001; Nishimura et al., 2003).

Raman tweezers is a powerful tool that provides fingerprints of biological cells of any kind in a short period of time. To date, this technique has been used to analyze single cells, such as yeast, red blood cells, bacteria, chromosomes, bacterial spores, red corals, and membrane components of cells (Ashkin, 1997; Chan et al., 2004; Kaczorowska et al., 2003; Puppels et al., 1990; Ramser et al., 2004; Sanderson and Ward, 2004; Xie and Li, 2003). This is the first time near-infrared Raman spectroscopy has been used to analyze the physiological relevance of virus infection.

Acknowledgements

This work was partly funded by an institutional research grant from American Cancer Society (IRG-97-149) to S.M.A. and by a Research/Creative Activity grant from East Carolina University to Y.L.

References

Ablashi, D.V., Chatlynne, L.G., Whitman Jr., J.E., Cesarman, E., 2002. Spectrum of Kaposi's sarcoma-associated herpesvirus, or human herpesvirus 8, diseases. Clin. Microbiol. Rev. 15, 439–464.

Akula, S.M., Ford, P.W., Whitman, A.G., Hamden, K.E., Bryan, B.A., Cook, P.P., McCubrey, J.A., 2005. B-Raf dependent expression of vascular endothelial growth factor-A in Kaposi's sarcoma-associated herpesvirus infected human B cells. Blood 105, 4516–4522.

Akula, S.M., Ford, P.W., Whitman, A.G., Hamden, K.E., Shelton, J.G., McCubrey, J.A., 2004. Raf promotes human herpesvirus-8 (HHV-8/KSHV) infection. Oncogene 23, 5227–5241.

Akula, S.M., Pramod, N.P., Wang, F.Z., Chandran, B., 2002. Integrin alpha3beta1 (CD 49c/29) is a cellular receptor for Kaposi's sarcoma-associated herpesvirus (KSHV/HHV-8) entry into the target cells. Cell 108, 407–419.

Aoki, Y., Tosato, G., 2001. Vascular endothelial growth factor/vascular permeability factor in the pathogenesis of primary effusion lymphomas. Leuk. Lymphoma 41, 229–237.

Ashkin, A., 1997. Optical trapping and manipulation of neutral particles using lasers. Proc. Natl. Acad. Sci. U.S.A. 94, 4853–4860.

Chan, J.W., Esposito, A.P., Talley, C.E., Hollars, C.W., Lane, S.M., Huser, T., 2004. Reagentless identification of single bacterial spores in aqueous solution by confocal laser tweezers Raman spectroscopy. Anal. Chem. 76, 599–603.

Chang, Y., Cesarman, E., Pessin, M.S., Lee, F., Culpepper, J., Knowles, D.M., Moore, P.S., 1994. Identification of herpesvirus-like DNA sequences in AIDS-associated Kaposi's sarcoma. Science 266, 1865–1869.

Davies, H., Bignell, G.R., Cox, C., Stephens, P., Edkins, S., Clegg, S., Teague, J., Woffendin, H., Garnett, M.J., Bottomley, W., Davis, N., Dicks, E., Ewing, R., Floyd, Y., Gray, K., Hall, S., Hawes, R., Hughes, J., Kosmidou, V., Menzies, A., Mould, C., Parker, A., Stevens, C., Watt, S., Hooper, S., Wilson, R., Jayatilake, H., Gusterson, B.A., Cooper, C., Shipley, J., Hargrave, D., Pritchard-Jones, K., Maitland, N., Chenevix-Trench, G., Riggins, G.J., Bigner, D.D., Palmieri, G., Cossu, A., Flanagan, A., Nicholson, A., Ho, J.W., Leung, S.Y., Yuen, S.T., Weber, B.L., Seigler, H.F., Darrow, T.L., Paterson, H., Marais, R., Marshall, C.J., Wooster, R., Stratton, M.R., Futreal, P.A., 2002. Mutations of the *BRAF* gene in human cancer. Nature 417, 949–954.

Ensoli, B., Sgadari, C., Barillari, G., Sirianni, M.C., Sturzl, M., Monini, P., 2001. Biology of Kaposi's sarcoma. Eur. J. Cancer 37, 1251–1269.

Faris, M., Ensoli, B., Stahl, N., Yancopoulos, G., Nguyen, A., Wang, S., Nel, A.E., 1996. Differential activation of the extracellular signal-regulated kinase, Jun kinase and Janus kinase-Stat pathways by oncostatin M and basic fibroblast growth factor in AIDS-derived Kaposi's sarcoma cells. AIDS 10, 369–378.

Gallo, R.C., 1998. HIV-1, HHV-8, and Kaposi's sarcoma. J. Hum. Virol. 1, 185–186.

Hamden, K.E., Ford, P.W., Whitman, A.G., Dyson, O.F., Cheng, S.Y., McCubrey, J.A., Akula, S.M., 2004. Raf-induced vascular endothelial growth factor augments Kaposi's sarcoma-associated herpesvirus infection. J. Virol. 78, 13381–13390.

Hamden, K.E., Whitman, A.G., Ford, P.W., Shelton, J.G., McCubrey, J.A., Akula, S.M., 2005. Raf and VEGF: emerging therapeutic targets in Kaposi's sarcoma-associated herpesvirus infection and angiogenesis in hematopoietic and nonhematopoietic tumors. Leukemia 19, 18–26.

Huang, W.E., Griffiths, R.I., Thompson, I.P., Bailey, M.J., Whiteley, A.S., 2004. Raman microscopic analysis of single microbial cells. Anal. Chem. 76, 4452–4458.

Ito, Y., Oike, Y., Yasunaga, K., Hamada, K., Miyata, K., Matsumoto, S., Sugano, S., Tanihara, H., Masuho, Y., Suda, T., 2003. Inhibition of angiogenesis and vascular leakiness by angiopoietin-related protein 4. Cancer Res. 63, 6651–6657.

Kaczorowska, B., Hacura, A., Kupka, T., Wrzalik, R., Talik, E., Pasterny, G., Matuszewska, A., 2003. Spectroscopic characterization of natural corals. Anal. Bioanal. Chem. 377, 1032–1037.

Karasarides, M., Chiloeches, A., Hayward, R., Niculescu-Duvaz, D., Scanlon, I., Friedlos, F., Ogilvie, L., Hedley, D., Martin, J., Marshall, C.J., Springer, C.J., Marais, R., 2004. B-RAF is a therapeutic target in melanoma. Oncogene 23, 6292–6298.

Kimura, E.T., Nikiforova, M.N., Zhu, Z., Knauf, J.A., Nikiforov, Y.E., Fagin, J.A., 2003. High prevalence of BRAF mutations in thyroid cancer: genetic evidence for constitutive activation of the RET/PTC-RAS-BRAF signaling pathway in papillary thyroid carcinoma. Cancer Res. 63, 1454–1457.

Lagunoff, M., Lukac, D.M., Ganem, D., 2001. Immunoreceptor tyrosine-based activation motif-dependent signaling by Kaposi's sarcoma-associated herpesvirus K1 protein: effects on lytic viral replication. J. Virol. 75, 5891–5898.

Liu, J., Wang, X.B., Park, D.S., Lisanti, M.P., 2002. Caveolin-1 expression enhances endothelial capillary tubule formation. J. Biol. Chem. 277, 10661–10668.

Mercer, K.E., Pritchard, C.A., 2003. Raf proteins and cancer: B-Raf is identified as a mutational target. Biochim. Biophys. Acta 1653, 25–40.

Neipel, F., Albrecht, J.C., Fleckenstein, B., 1997. Cell-homologous genes in the Kaposi's sarcoma-associated rhadinovirus human herpesvirus 8: determinants of its pathogenicity? J. Virol. 71, 4187–4192.

Nishimura, K., Ueda, K., Sakakibara, S., Do, E., Ohsaki, E., Okuno, T., Yamanishi, K., 2003. A viral transcriptional activator of Kaposi's sarcoma-associated herpesvirus (KSHV) induces apoptosis, which is blocked in KSHV-infected cells. Virology 316, 64–74.

Puppels, G.J., de Mul, F.F., Otto, C., Greve, J., Robert-Nicoud, M., Arndt-Jovin, D.J., Jovin, T.M., 1990. Studying single living cells and chromosomes by confocal Raman microspectroscopy. Nature 347, 301–303.

Ramser, K., Logg, K., Goksor, M., Enger, J., Kall, M., Hanstorp, D., 2004. Resonance Raman spectroscopy of optically trapped functional erythrocytes. J. Biomed. Opt. 9, 593–600.

Renne, R., Blackbourn, D., Whitby, D., Levy, J., Ganem, D., 1998. Limited transmission of Kaposi's sarcoma-associated herpesvirus in cultured cells. J. Virol. 72, 5182–5188.

Russo, J.J., Bohenzky, R.A., Chien, M.C., Chen, J., Yan, M., Maddalena, D., Parry, J.P., Peruzzi, D., Edelman, I.S., Chang, Y., Moore, P.S., 1996. Nucleotide sequence of the Kaposi sarcoma-associated herpesvirus (HHV8). Proc. Natl. Acad. Sci. U.S.A. 93, 14862–14867.

Sanderson, J.M., Ward, A.D., 2004. Analysis of liposomal membrane composition using Raman tweezers. Chem. Commun. (Camb.), 1120–1121.

Weinstein-Oppenheimer, C., Burrows, C., Steelman, L., McCubrey, J., 2002. The effects of beta-estradiol on Raf activity, cell cycle progression and growth factor synthesis in the MCF-7 breast cancer cell line. Cancer Biol. Ther. 1, 256–262.

Xie, C., Dinno, M.A., Li, Y.Q., 2002. Near-infrared Raman spectroscopy of single optically trapped biological cells. Opt. Lett. 27, 249–251.

Xie, C., Li, Y.Q., 2003. Confocal micro-Raman spectroscopy of single biological cells using optical trapping and shifted excitation difference techniques. J. Appl. Phys. 93, 2982–2986.

Zhang, S., Nonoyama, M., 1994. The cellular proteins that bind specifically to the Epstein–Barr virus origin of plasmid DNA replication belong to a gene family. Proc. Natl. Acad. Sci. U.S.A. 91, 2843–2847.